

Intermittent release of transients in the slow solar wind: 2. In situ evidence

Article

Published Version

Rouillard, A. P., Lavraud, B., Davies, J. A., Savani, N. P., Burlaga, L. F., Forsyth, R. J., Sauvaud, J.-A., Opitz, A., Lockwood, M. ORCID: <https://orcid.org/0000-0002-7397-2172>, Luhmann, J. G., Simunac, K. D. C., Galvin, A. B., Davis, C. J. ORCID: <https://orcid.org/0000-0001-6411-5649> and Harrison, R. A. (2010) Intermittent release of transients in the slow solar wind: 2. In situ evidence. *Journal of Geophysical Research*, 115. A04104. ISSN 0148-0227 doi: 10.1029/2009JA014472 Available at <https://centaur.reading.ac.uk/7207/>

It is advisable to refer to the publisher's version if you intend to cite from the work. See [Guidance on citing](#).

Published version at: <http://dx.doi.org/10.1029/2009JA014472>

To link to this article DOI: <http://dx.doi.org/10.1029/2009JA014472>

Publisher: American Geophysical Union

All outputs in CentAUR are protected by Intellectual Property Rights law, including copyright law. Copyright and IPR is retained by the creators or other copyright holders. Terms and conditions for use of this material are defined in the [End User Agreement](#).

www.reading.ac.uk/centaur

CentAUR

Central Archive at the University of Reading

Reading's research outputs online

Intermittent release of transients in the slow solar wind:

2. In situ evidence

A. P. Rouillard,^{1,2,3,4} B. Lavraud,^{3,4} J. A. Davies,² N. P. Savani,⁵ L. F. Burlaga,⁶
R. J. Forsyth,⁵ J.-A. Sauvaud,^{3,4} A. Opitz,^{3,4} M. Lockwood,^{1,2} J. G. Luhmann,⁷
K. D. C. Simunac,⁸ A. B. Galvin,⁸ C. J. Davis,² and R. A. Harrison²

Received 19 May 2009; revised 9 September 2009; accepted 21 October 2009; published 10 April 2010.

[1] In paper 1, we showed that the Heliospheric Imager (HI) instruments on the pair of NASA STEREO spacecraft can be used to image the streamer belt and, in particular, the variability of the slow solar wind which originates near helmet streamers. The observation of intense intermittent transient outflow by HI implies that the corresponding in situ observations of the slow solar wind and corotating interaction regions (CIRs) should contain many signatures of transients. In the present paper, we compare the HI observations with in situ measurements from the STEREO and ACE spacecraft. Analysis of the solar wind ion, magnetic field, and suprathermal electron flux measurements from the STEREO spacecraft reveals the presence of both closed and partially disconnected interplanetary magnetic field lines permeating the slow solar wind. We predict that one of the transients embedded within the second CIR (CIR-D in paper 1) should impact the near-Earth ACE spacecraft. ACE measurements confirm the presence of a transient at the time of CIR passage; the transient signature includes helical magnetic fields and bidirectional suprathermal electrons. On the same day, a strahl electron dropout is observed at STEREO-B, correlated with the passage of a high-plasma beta structure. Unlike ACE, STEREO-B observes the transient a few hours ahead of the CIR. STEREO-A, STEREO-B, and ACE spacecraft observe very different slow solar wind properties ahead of and during the CIR analyzed in this paper, which we associate with the intermittent release of transients.

Citation: Rouillard, A. P., et al. (2010), Intermittent release of transients in the slow solar wind: 2. In situ evidence, *J. Geophys. Res.*, 115, A04104, doi:10.1029/2009JA014472.

1. Introduction

[2] The slow and fast solar wind differ in several ways; the values and variances of their bulk properties (densities, velocities and temperatures) and their respective composition. The slow solar wind is denser and colder than the fast solar wind [Snyder *et al.*, 1963] and both the density and temperature of the slow solar wind measured in situ are

highly variable with a 40% variance at $\sim 300 \text{ km s}^{-1}$ [Zurbuchen *et al.*, 2002]. The clear distinction between the fast and slow solar wind is less obvious in regions where they interact [Burlaga and Szabo, 1999]. The origin of the slow solar wind is therefore most probably different to that of the fast solar wind. The different composition of the slow and fast solar wind [Geiss *et al.*, 1995a, 1995b; Zurbuchen *et al.*, 1999] has been related to reconnection occurring between open magnetic field lines and photospheric magnetic loops [Fisk, 1996; Schwadron *et al.*, 1999] or to the different coronal heights at which waves deposit energy for fast and slow solar wind [Wang *et al.*, 2009].

[3] Helmet streamers are particularly interesting structures of the lower corona. These comprise open field lines lying over closed magnetic loops of the photosphere. When adjacent open field lines are of opposite polarity, they can reconnect, leading to their complete disconnection [Wang *et al.*, 2000; van Aalst *et al.*, 1999]. The underlying regions of the helmet streamers are permeated by closed loops which can reconnect with one another creating helical fields [Gosling *et al.*, 1995], or simply forming larger loops released in the solar wind [Wang and Sheeley, 2003]. The closed loops of the underlying layers of the helmet streamers

¹Space Environment Physics Group, School of Physics and Astronomy, University of Southampton, Southampton, UK.

²Space Science and Technology Department, Rutherford Appleton Laboratory, Chilton, UK.

³Universit  de Toulouse, UPS, Centre d'Etude Spatiale des Rayonnements, Toulouse, France.

⁴UMR 5187, Centre National de la Recherche Scientifique, Toulouse, France.

⁵Space and Atmospheric Physics, Blackett Laboratory, Imperial College London, London, UK.

⁶NASA Goddard Space Flight Center, Greenbelt, Maryland, USA.

⁷Space Science Laboratory, University of California, Berkeley, California, USA.

⁸Institute for the Study of Earth Oceans and Space, University of New Hampshire, Durham, New Hampshire, USA.

Table 1. Trajectories of the Transients Determined From HI-A Observations of CIR-D^a

Transient	Date	Time (UT)	V_r (km s ⁻¹)	$\Delta\beta$ (ACE, T) (deg)	$\Delta\beta$ (B, T) (deg)	Impact?
a	9 Sep	0107	268 ± 14	68 ± 04	55 ± 04	no
b	9 Sep	1945	288 ± 24	66 ± 09	53 ± 09	no
c	10 Sep	0657	285 ± 16	62 ± 10	49 ± 10	no
d	10 Sep	2139	299 ± 11	47 ± 11	34 ± 11	no
e	11 Sep	0752	311 ± 18	45 ± 11	32 ± 11	no
f	11 Sep	2019	335 ± 07	21 ± 07	08 ± 07	no

^aShown are the date that the transient passed 5° of elongation, the estimated speed of the transient (V_r), the angular separation in ecliptic longitude between STEREO-A and ACE and between STEREO-A and STEREO-B, and predicted impacts.

can also reconnect with the open field lines of the overlying layers leading to foot point exchange [Wang *et al.*, 2000]. The band of slow solar wind, called the streamer belt, is formed by plasma streaming along the open field lines of helmet streamers. Consequently, the high variability of the slow solar wind may result from the continual activity of the helmet streamers.

[4] In situ observations of the slow solar wind provide evidence for the occurrence of foot point exchange, field line disconnection and the emergence of closed loops inside and near helmet streamers. High-plasma beta structures associated with refolded magnetic field lines have been explained as “fossilized” signatures of foot point exchange occurring at the coronal base [Crooker *et al.*, 2004; Zurbuchen *et al.*, 2002]. The disappearance of the field-aligned strahl is frequently observed in situ and may result from either complete disconnection of open field lines near the Sun or interchange reconnection [Gosling *et al.*, 2005; Pagel *et al.*, 2005]. Kilpua *et al.* [2009] have observed frequent periods of counterstreaming electrons in the slow solar wind during the current solar minimum that could be related to the observation of magnetic field lines connected at each end to the solar surface (i.e., closed loops).

[5] Transients in the streamer belt region have been observed for more than a decade by the Large Angle Spectrometric Coronagraph (LASCO) coronagraph on the Solar and Heliospheric Observatory (SOHO), as described in paper 1 [see also Wang *et al.*, 1998, 2000], and are now being imaged by the Sun Earth Connection Coronal and Heliospheric Investigation (SECCHI) package on the two Solar Terrestrial Relations Observatory (STEREO) spacecraft (see paper 1 and references therein).

[6] This paper aims to answer two questions. The first is does the slow solar wind observed in situ by STEREO-A/B and the ACE spacecraft, during the periods of enhanced variable outflows imaged by SECCHI, contain recognizable signatures of transients? If the answer is yes, are the tracks observed clearly by the outermost cameras of the STEREO Heliospheric Imager (HI) transients entrained by CIRs, as suggested in paper 1?

2. Instruments

[7] In addition to the SECCHI imaging suite described in paper 1, each of the STEREO spacecraft also carries a comprehensive suite of in situ instrumentation, including the

Plasma and Suprathermal Ion Composition (PLASTIC) [Galvin *et al.*, 2008] and the In Situ Measurements of Particles and CME Transients (IMPACT) [Luhmann *et al.*, 2008] packages. Magnetic field measurements from the magnetometer (MAG) [Acuña *et al.*, 2008] and suprathermal electron observations from the Solar Wind Electron Analyzer (SWEA) [Sauvaud *et al.*, 2008], two components of the IMPACT package, are used in the present study together with the solar wind ion moments derived from measurements made by the PLASTIC package. In situ measurements of near-Earth solar wind electron and ion as well as suprathermal electrons made by the Solar Wind Electron, Proton, Alpha Monitor investigation (SWEPAM) [McComas *et al.*, 1998], solar wind composition measured by the Solar Wind Ion Composition Spectrometer and the Solar Wind Ion Mass Spectrometer (SWICS/SWIS) [Gloeckler *et al.*, 1998] and measurements of the magnetic field by the magnetic field investigation (MAG) [Smith *et al.*, 1998] on board the Advanced Composition Explorer (ACE) are also used in the present paper. As we shall see, the combination of the STEREO-A and -B spacecraft and ACE form an ideal constellation of spacecraft to study solar wind structures near 1 AU.

3. Predicted Transient Impacts

[8] In paper 1, we presented evidence of intermittent plasma release from a corotating source as imaged by STEREO HI. In the following analysis, we use the fitting of transient tracks in the J-maps from paper 1 to determine if any of these transients could have been detected in situ. The frequency of the release of the transients by helmet streamers (every few hours) and their limited longitudinal extent (likely <10°) suggest that a transient measured in situ by one STEREO spacecraft is likely not to be observed in situ by either the other STEREO spacecraft or ACE; the longitudinal extent of these small transients is probably smaller than the minimum angular separation between the three spacecraft during September 2007 (14°). September 2007 was marked by a profusion of tracks in the J-maps derived from the HI images (see paper 1), which is indicative of high streamer activity. As a consequence, the slow solar wind measured in situ by STEREO-A, B and ACE in the vicinity of CIRs is expected to contain signatures of small transient events swept up into the CIR.

[9] Three different CIRs were imaged by HI on STEREO-A and -B (see paper 1) and up to 6 transients were observed to be entrained within each CIR. However, only one CIR was imaged continuously by the HI cameras on both STEREO-A and STEREO-B; we present the in situ analysis of this CIR in the present paper (i.e., CIR-D from paper 1). From Tables 1 and 2 of paper 1 we can determine if any of the transient would be expected to impact ACE, STEREO-A or STEREO-B during the CIR passage. Tables 1 and 2 of paper 1 are partially reproduced and extended in Tables 1 and 2 of the present paper. The label, time at 5° elongation, and estimated speed of the transients imaged by HI on STEREO-A are given in Table 1. The angles of propagation of each transient relative to ACE ($\Delta\beta$ (ACE,T)) and STEREO-B ($\Delta\beta$ (B,T)) are also shown. An impact with either spacecraft is expected when the angle of propagation of the transient relative to that spacecraft is zero or consistent

Table 2. Same as Table 1 but for Observations of Transients Imaged by HI on STEREO-B^a

Transient	Date	Time (UT)	V_r (km s ⁻¹)	$\Delta\beta$ (ACE, T) (deg)	$\Delta\beta$ (A, T) (deg)	Impact?
d	16 Sep	2031	357 ± 90	0 ± 15	17 ± 15	ACE
e	17 Sep	0952	333 ± 15	22 ± 09	05 ± 09	A (WE)
f	18 Sep	0943	274 ± 05	45 ± 10	28 ± 10	no
g	20 Sep	0520	319 ± 10	71 ± 07	54 ± 07	no

^aWE stands for impact within error.

with zero within error (WE) limits. The “Impact?” entries in Table 1 show that none of the transients mapped by STEREO-A was predicted to impact ACE or STEREO-B.

[10] Table 2 shows that transient d of CIR-D imaged by HI on STEREO-B is predicted to directly impact ACE. Within the uncertainty of the trajectory estimate, we find that transient e imaged by HI-B may have impacted STEREO-A. Transient d is the only transient entrained by CIR-D predicted to directly impact a spacecraft (ACE). Transient d was located at an elongation of 5° in the HI-1B images at 2000 UT on 16 September. This elongation corresponds to a coronal height of 0.28 AU (obtained from equation 2 of paper 1 with $\alpha_0 = 5^\circ$ and $\beta = 17^\circ$ relative to STEREO-B). The predicted speed of transient d was 357 km s⁻¹; we therefore predict an impact at ACE (~1 AU) on 20 September at ~0900 UT.

[11] The impact predictions are limited by how well the entrained transients are observed by the HI cameras. The results presented in Tables 1 and 2 of paper 1 show that the HI cameras on STEREO-B, HI-B, have a greater tendency than the HI-A cameras to observe transients propagating with small longitudinal separation angles (β). A physical explanation for this effect may rely on the orientation of the transient relative to the line of sight. Figure 1 of paper 1 presents typical Archimedian spirals along which the CIR-associated density pileup usually develops. Three arbitrary lines of sight are shown in Figures 1a and 1b of this paper, the HI-A and HI-B fields of view, respectively. The integrated white-light signal detected by HI-A should be enhanced along the Archimedian spiral during observations of CIR propagation at large rather than small longitude angles relative to the spacecraft. In contrast, the HI-B cameras will integrate light scattered over a greater portion of the CIR spiral for small β angles (see Rouillard *et al.* [2009a] for a more detailed description of this effect). This effect has been modeled using ray-tracing techniques, including the effect of Thomson scattering, for the HI fields of view [see, e.g., Howard *et al.*, 2008]. The list of fitted transients presented in Table 1 or 2 is limited by the geometry of the observed interplanetary events. Transients may have been passing through the STEREO-A (B) HI images undetected and yet may have impacted ACE or STEREO-B (A). Section 4 presents a discussion of the in situ observations in terms of these predictions.

4. In Situ Observations of CIR-D

[12] Figure 2 presents in situ observations of the solar wind recorded at STEREO-B, ACE and STEREO-A during

the passage of CIR-D. Typical CIR signatures are observed at all spacecraft, a characteristic increase in solar wind speed (Figures 2e, 2m, and 2u), magnetic field strength (Figures 2b, 2j, and 2r), and density (Figures 2f, 2n, and 2v). The stream interface (SI) for CIR-D, where slow, cold solar wind is followed by fast solar wind [Burlaga, 1974; Gosling *et al.*, 1976], determined for the three spacecraft is marked in Figure 2. STEREO-B, ACE and STEREO-A were located at heliographic latitudes of 7.3, 7.1 and 6.5°, respectively, and therefore sampled different parts of the same CIR. Helios observations have revealed that a latitudinal separation of only 1° between two spacecraft can lead to significant observational differences as they observe different latitudinal slices through the same coronal hole [Schwenn and Marsch, 1990]. Rouillard *et al.* [2009a] presented such observations of a latitudinal variation in the solar wind speed of a CIR observed by the STEREO and ACE spacecraft in July 2007. In the present study, STEREO-B, ACE and STEREO-A were located at Carrington longitudes 277.7, 291.9 and 309.1°, respectively, which corresponds to a minimum longitudinal separation of 14° between any spacecraft. Opitz *et al.* [2009] showed, using STEREO in situ data, that after adjusting for spacecraft location, the correlation between solar wind bulk velocity measurements at STEREO-A and STEREO-B decreased with increasing time difference. Hence some of the interspacecraft differences between in situ observations of CIR-D presented here will be related to spatial and temporal variations in the CIR.

[13] The magnetic field azimuth fluctuated around 135° before and after the CIR passage (Figures 2c, 2k, and 2s).

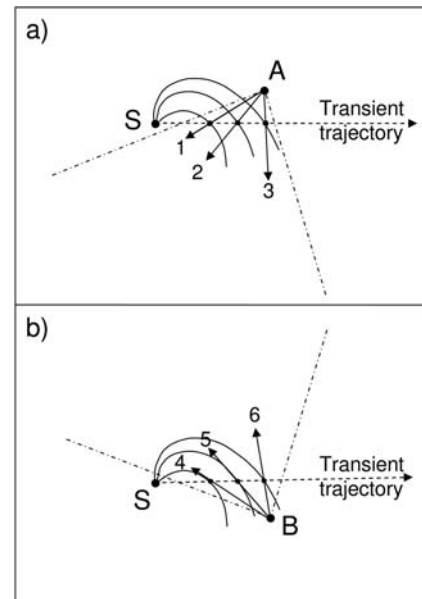


Figure 1. (a) A schematic of the ecliptic plane viewed from above showing the position of the Sun (S) and STEREO-A (A). A transient trajectory at a small longitude difference with respect to STEREO-A is shown as a dashed black line. The transient is observed at three successive times along directions 1, 2, and 3. (b) The same format as Figure 1a but for observations made by STEREO-B.

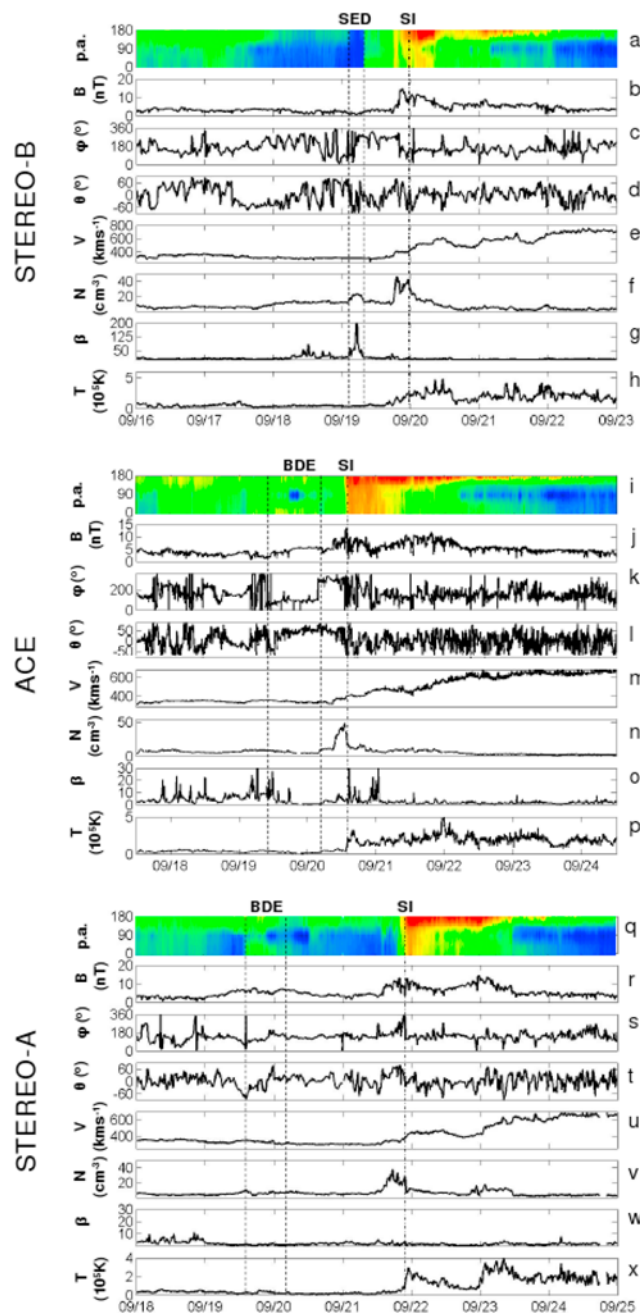


Figure 2. In situ data measured during the passage of CIR-D. (a, i, q) The 250 eV and 272 eV electron pitch angle (p.a.) distributions recorded by the STEREO and ACE spacecraft, respectively. (b, j, r) Magnetic field strength (B), (c, k, s) azimuth (ϕ), and (d, l, t) elevation (θ). (e, m, u) Speed (V), (f, n, v) density (N), (g, o, w) plasma beta (β), and (h, p, x) temperature (T) derived from solar wind ion data. Vertical dashed lines bound the periods of bidirectional electrons (BDEs) and strahl electron dropout (SED). The stream interface (SI) is shown for each spacecraft by a vertical line crossing all the plots.

The pitch angle distribution of suprathermal electrons (250 eV for STEREO-A/B and - 272 eV for ACE) shown in Figures 2a, 2i, and 2q can be used to study the connec-

tivity of interplanetary magnetic field lines with the solar surface [e.g., *Gosling et al.*, 2005; *Owens et al.*, 2008]. Solar wind electrons can be typically classified into three distinct populations. The main component corresponds to the thermal core electrons representing 95% of the total electron density. The remaining 5% comprises the suprathermal non-Maxwellian halo, distributed isotropically in velocity space, and the strahl. The strahl is mostly aligned in the direction parallel to the interplanetary magnetic field and, largely, moves away from the Sun [*Feldman et al.*, 1975; *Pilipp et al.*, 1987a, 1987b; *Owens et al.*, 2008]. The pitch angle of the strahl electrons does not change before and after the CIR passage (remaining at 180°) which shows that none of the three spacecraft crossed the HCS.

[14] There are no signatures of high-beta structures (Figure 2w), long-lasting directional changes in the magnetic field (Figures 2s and 2t) nor unusual pitch angle variations (Figure 2q) associated with the passage of CIR-D over STEREO-A. Of interest, however, is a period of bidirectional suprathermal electron (BDE) fluxes two days before the CIR arrival at STEREO-A (19 September at 1200 UT) lasting 12 h (Figure 2q). These BDEs could be related to the passage of closed magnetic field lines over the STEREO-A spacecraft [*Gosling et al.*, 1987]. This transient signature is observed in the slow solar wind well ahead of the CIR and so it was therefore not entrained by the CIR. Moreover, as it is not associated with a significant density increase, it did not have an associated white-light signature in the HI images. The predictions in Table 2 show that transient e entrained by CIR-D ($5 \pm 9^\circ$) may have impacted STEREO-A; however, no clear in situ signature is observed. The transient may have just missed the spacecraft.

[15] As well as observing the same CIR-associated density enhancement seen in situ at STEREO-A, STEREO-B measures an additional density increase, 12 h before the arrival of the CIR (0600 UT on 19 September), again inside the slow solar wind region. This region of denser plasma is not correlated with an increase in magnetic field strength but rather a drop in field strength (Figure 2b) and is therefore marked by a very high plasma beta (Figure 2g). This feature is coincident with a local reversal in both the magnetic field azimuth and elevation (Figure 2c) and its passage is also marked by a significant dropout in strahl electrons of 250 eV electrons. Such a feature is termed a strahl electron dropout (SED) and is associated with the disappearance of the field-aligned strahl. SEDs are frequently observed in situ and are a phenomenon indicative of the passage of magnetic field lines that may have reconnected near the Sun (and indeed may be disconnected from the Sun) [*McComas et al.*, 1989; *Gosling et al.*, 2005; *Pagel et al.*, 2005; *Crooker and Pagel*, 2008]. The density increase associated with this transient structure is about a third of the later CIR-associated density increase. However, no clear track in Table 1 can be associated with it. From its in situ speed and angle of propagation, we predict that a density increase associated with this SED should appear in the HI-1A images on 15 September. HI J-maps from STEREO-A presented in Figure 9 of paper 1 do reveal that two tracks appeared on that day. These tracks faded away very quickly and could therefore not be fitted accurately to estimate the transient's trajectories. The latter structures are probably that of transients which have not been

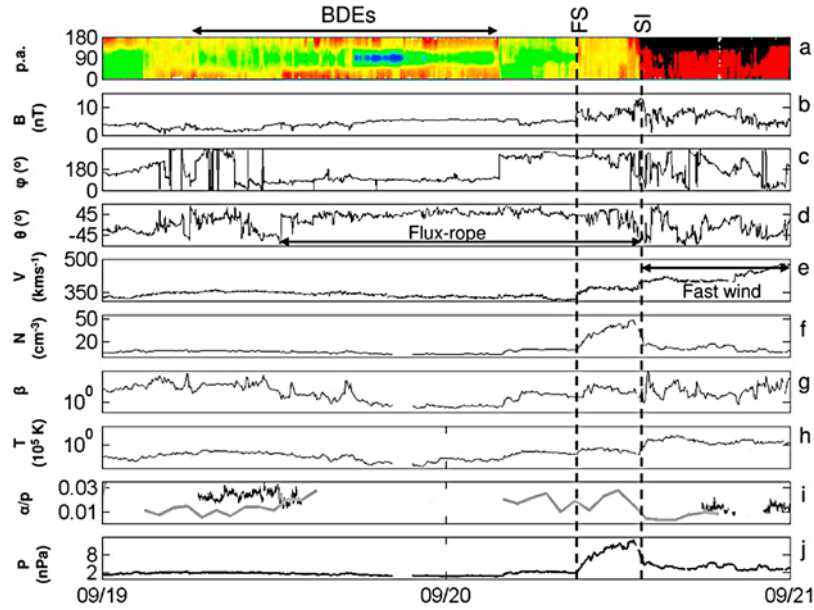


Figure 3. Figures 3a–3h present a 48 h subset interval of the time variation of solar wind parameters presented in Figures 2i–2p. Additionally, Figure 3i presents the time variation of the alpha to proton ratio (black line) measured by SWEAPM and the O7+/O6+ ratio (divided by 5) measured by ACE-SWICS/SWIMS (grey line). Figure 3j shows the total solar wind pressure (P (nPa)). The extent of the flux rope located on the antisunward flank of the SI is indicated together with the time interval of BDEs and the passage of a forward shock (FS).

swept up by CIRs. We cannot thus make a clear association with the SED observed in situ.

[16] Signatures of a typical CIR passage are observed at ACE around 20 September, with a clearly identifiable SI. The suprathermal electron pitch angle distribution is particularly interesting as a clear period of BDEs can be observed on 19 September at 0600 UT, lasting nearly 24 h. Figure 3 presents a subset of the ACE data shown in Figure 2 covering the interval during which ACE observed the BDEs in the slow solar wind. The very low electron fluxes at 90° around 2000 UT on 19 September are likely related to Halo depletion at 90° pitch angle commonly found within CMEs [Gosling *et al.*, 2001, 2002]. A period of low plasma beta and solar wind temperature accompanied by rotating magnetic fields and increase in field strength satisfies the conditions set by Burlaga *et al.* [1981] to classify it as a magnetic cloud (MC).

[17] A force-free field fit to the magnetic field inside the magnetic cloud (MC) is used to determine whether the period of significant out-of-ecliptic magnetic fields and strong BDEs observed at ACE is associated with the passage of a flux rope; the fitting technique is the same as that used by Rees and Forsyth [2004]. The azimuth, elevation and strength of the magnetic field was successfully fitted by a force-free field. The fitted flux rope is found to have right-handed chirality, and the MC axis orientation in Radial Tangential Normal (RTN) coordinates is found to be approximately $(-0.25, 0.12, 0.96)$. This orientation corresponds to a cloud axis orthogonal to the RT plane (i.e., a nearly vertical flux rope), and 25° from the nominal azimuth angle of the background Parker spiral field ($\bar{\phi} = 135^\circ$, $\bar{\phi} =$

315°). The force-free field fit could not be extended beyond 1400 UT on 20 September, as this time marks the SI crossing and passage into the fast solar wind.

[18] The ACE spacecraft passed through a small MC at the predicted arrival time of transient d. The entire MC does not appear to have a closed topology as the BDEs cease several hours before the end of the MC (determined by the end of the field rotation in Figure 3d). This is not unusual and is probably related to the occurrence of partial magnetic reconnection at one foot point of the flux rope near to the Sun [Crooker *et al.*, 2008; Rouillard *et al.*, 2009a]. The speed of the magnetic cloud decreases from 350 to 320 km s^{-1} as it passes over ACE suggesting that it is expanding along the radial direction. This is commonly observed in in situ measurements [Klein and Burlaga, 1982; Lepping *et al.*, 2008; Owens, 2006] and recently in white-light observations made by HI [Rouillard *et al.*, 2009b; Davis *et al.*, 2009]. Figure 3i presents the $\text{He}^{++}/\text{H}^+$ ratio (black line) and the $\text{O}^{7+}/\text{O}^{6+}$ charge state ratio (grey line: the ratio was divided by 5 to facilitate comparison). Magnetic clouds are often enriched in the ratio $\text{He}^{++}/\text{H}^+$ and $\text{O}^{7+}/\text{O}^{6+}$ [Hirshberg *et al.*, 1972; Neugebauer and Goldstein, 1997; Zurbuchen *et al.*, 2002]. Unfortunately, there are large data gaps during the interval shown in Figure 3i; however, the ratios are enhanced when ACE enters the MC. A few hours later, the ratio of $\text{O}^{7+}/\text{O}^{6+}$ drops from >0.1 to 0.04 when ACE exits the MC to enter the CIR flows. The region of interaction between the MC and the CIR, located on the sunward flank of the SI, is marked by an increased solar wind density and the presence of a forward shock (FS). CIR-associated shocks are rarely observed inside of 1 AU, it is likely both

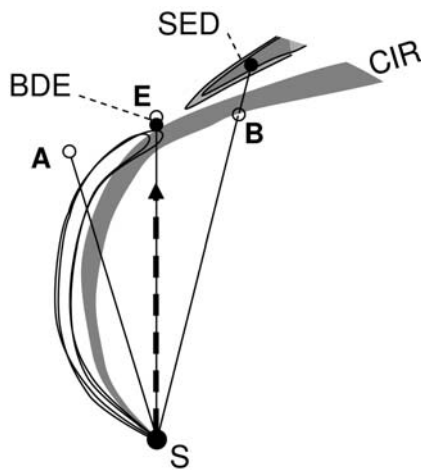


Figure 4. The position of STEREO-A (A), Earth (E), STEREO-B (B), and the Sun (S) shown for 19 September 2007. The plasma compressed by a CIR is marked as a grey spiral. The connected/disconnected parts of the fields swept up by the CIR are also shown together with their associated BDEs and SEDs.

that part of the increased density behind the FS and the FS itself resulted from the magnetic cloud expanding into the region of compression. This region of interaction marks the region where the CIR and the transient (comprising a complex system of closed and partially open field lines) interact to form a denser structure. Interestingly, the total density increase associated with CIR-D is greater at ACE than at STEREO-A or STEREO-B which supports the idea that the interaction of the MC and the CIR forced a local increase in density. The predicted time of impact of transient d at ACE on 20 September at around 0900 UT corresponds precisely to the region of interaction of the MC with the CIR. The speed of transient d predicted from the HI images, 357 km s^{-1} , agrees very well with a speed of 340 km s^{-1} measured in situ inside the region of MC-CIR interaction. We therefore relate the observations of an entrained transient d by HI-2B directly to this CIR-MC interaction.

5. Discussion and Conclusion

[19] This second paper presented an analysis of in situ observations of a CIR (CIR-D from paper 1) which entrained transients at or near the longitudes of either STEREO-A, STEREO-B or ACE. CIR-D was predicted from HI images to entrain at least one spacecraft-impacting transient. Impact is confirmed by the ACE in situ observations. We associate the HI observations of transient d (Table 2) directly to the interaction of an expanding magnetic cloud into CIR-D. The MC was not associated with an increase in plasma density ahead of the flux rope, which suggests that HI could not detect the leading edge of the transient as it progressed through the interplanetary medium. Multiplying the average speed of the ICME (330 km s^{-1}) by the duration of CME passage ($\sim 24 \text{ h}$), one finds an ICME radial size of roughly 0.2 AU ; this size is typical of ICMEs at 1 AU . Yet no clear ICME onset were observed in the solar data; no flare, filament eruption nor EUVI waves were observed in particular.

[20] Figure 4 presents a possible sequence of events which may have led to the observations of SEDs and BDEs at the ACE and STEREO spacecraft. In this scenario, a connected-disconnected bundle of magnetic field lines is released from the Sun and convected outward in the slow solar wind. The MC is entrained by the CIR roughly along the longitude of the Earth leading to a local increase in the CIR density. The STEREO-B spacecraft observed primarily the SED associated with the disconnected field lines which may or may not be related to the MC seen at ACE.

[21] We note that transients which are continually released in the slow solar wind but are not swept up by a/the CIR will leave a strong signal at the sunward edge of the HI-1 images but these will fade away quickly as they are not entrained and do not interact with the CIR. Such features are probably seen in the J-maps from both HI-1A and HI-1B as the ephemeral increases in coronal brightness (described in paper 1) that are visible only out to elongation of less than 10° . The SED observed at STEREO-B ahead of CIR-D may well have been associated with one of these short-lived brightness increases at the coronal base. The sequence of events at CIR-C (see paper 1), although not shown here, provides supplementary information on the condition of the slow solar wind during the period of frequent transient releases observed by the HI instrument. Additional transients were observed in situ in the slow solar wind, including BDE events associated with the passage of closed field lines. High plasma beta structures, marked by temporary reversals of the field line orientation, were also observed in the slow solar wind ahead of CIR-C. Hence these additional observations support the presence of frequent transients in the slow solar wind. The presence of partially disconnected field lines, refolded field lines and closed magnetic field lines have been inferred from numerous studies of the slow solar wind observed both in situ and in white light [Wang *et al.*, 1998; Crooker *et al.*, 1993; Zurbuchen *et al.*, 2002]. This study provides the first direct link between these streamer events and the transients observed in the slow solar wind by previous authors. Rouillard *et al.* [2009a] present a case of a small magnetic cloud entrained by solar wind streams during July 2007 while Kilpua *et al.* [2009] find evidence of closed field lines permeating a significant fraction of the slow solar wind. All in situ observations of entrained streamer blobs have so far shown that they are magnetic clouds with helical topology [Rouillard *et al.*, 2009a]. Recently Sheeley *et al.* [2009] presented evidence for streamer blobs possessing flux rope topologies, this latter study provides additional evidence for frequent helical magnetic fields expelled by helmet streamers.

[22] It would be very interesting to carry out additional in situ statistical studies of the emergence of helical fields inside the slow solar wind and on the boundary of coronal holes in the manner of Cartwright and Moldwin [2008]. It is clear from the HI observations that transients are continually emitted, even during these years of extremely low activity and it is yet unclear what the role of helical fields and other magnetic structure plays for the long-term evolution of the coronal field [Lockwood *et al.*, 1999; Rouillard *et al.*, 2007; Owens *et al.*, 2007].

[23] **Acknowledgments.** This work was funded by the Science and Technology Facilities Council (UK). The STEREO/SECCHI data are pro-

duced by a consortium of RAL (UK), NRL (USA), LMSAL (USA), GSFC (USA), MPS (Germany), CSL (Belgium), IOTA (France), and IAS (France). The STEREO/SECCHI data were obtained from the World Data Center, Chilton, UK. The PLASTIC and IMPACT data are produced by a consortium of the CESR (France), the University of New Hampshire, and the University of California. The in situ data presented in this paper were partly obtained from the UKSSDC World Data Center, Chilton, UK.

[24] Zuyin Pu thanks Andy Breen and another reviewer for their assistance in evaluating this paper.

References

- Acuña, M. H., D. Curtis, J. L. Scheifele, C. T. Russell, P. Schroeder, A. Szabo, and J. G. Luhmann (2008), The STEREO/IMPACT magnetic field experiment, *Space Sci. Rev.*, **136**(1–4), 203–226.
- Burlaga, L. F. (1974), Interplanetary stream interfaces, *J. Geophys. Res.*, **79**, 3717–3725.
- Burlaga, L. F., and S. Szabo (1999), Fast and slow flows in the solar wind near the ecliptic at 1 AU, *Space Sci. Rev.*, **87**(1–2), 137–140.
- Burlaga, L. F., E. Sittler, F. Mariani, and R. Schwenn (1981), Magnetic loop behind an interplanetary shock: Voyager, Helios, and IMP 8 observations, *J. Geophys. Res.*, **86**, 6673–6684.
- Cartwright, M. L., and M. B. Moldwin (2008), Comparison of flux rope magnetic properties to large-scale magnetic clouds: Evidence for reconnection across the HCS?, *J. Geophys. Res.*, **113**, A09105, doi:10.1029/2008JA013389.
- Crooker, N. U., and C. Pagel (2008), Residual strahls in solar wind electron dropouts: Signatures of magnetic connection to the Sun, disconnection, or interchange reconnection?, *J. Geophys. Res.*, **113**, A02106, doi:10.1029/2007JA012421.
- Crooker, N. U., G. L. Siscoe, S. Shodhan, D. F. Webb, J. T. Gosling, and E. J. Smith (1993), Multiple heliospheric current sheets and coronal streamer belt dynamics, *J. Geophys. Res.*, **98**(A6), 9371–9381.
- Crooker, N. U., M. E. Burton, J. L. Phillips, E. J. Smith, and A. Balogh (1996), Heliospheric plasma sheets, *J. Geophys. Res.*, **101**(A2), 2467–2474.
- Crooker, N. U., C.-L. Huang, S. M. Lamassa, D. E. Larson, S. W. Kahler, and H. E. Spence (2004), Heliospheric plasma sheets, *J. Geophys. Res.*, **109**, A03107, doi:10.1029/2003JA010170.
- Crooker, N. U., S. W. Kahler, J. T. Gosling, and R. P. Lepping (2008), Evidence in magnetic clouds for systematic open flux transport on the Sun, *J. Geophys. Res.*, **113**, A12107, doi:10.1029/2008JA013628.
- Davis, C. J., J. A. Davies, M. Lockwood, A. P. Rouillard, C. J. Eyles, and R. A. Harrison (2009), Stereoscopic imaging of an Earth-impacting solar coronal mass ejection: A major milestone for the STEREO mission, *Geophys. Res. Lett.*, **36**, L08102, doi:10.1029/2009GL038021.
- Feldman, W. C., J. R. Asbridge, S. J. Bame, M. D. Montgomery, and S. P. Gary (1975), *J. Geophys. Res.*, **80**(31), 4181–4196.
- Fisk, L. A. (1996), Motion of the footpoints of heliospheric magnetic field lines at the Sun: Implications for recurrent energetic particle events at high heliographic latitudes, *J. Geophys. Res.*, **101**(A7), 15,547–15,553.
- Galvin, A. B., et al. (2008), The Plasma and Suprathermal Ion Composition (PLASTIC) investigation on the STEREO observatories, *Space Sci. Rev.*, **136**(1–4), 437–486.
- Geiss, J., G. Gloeckler, and R. von Steiger (1995a), Origin of the solar wind from composition data, *Space Sci. Rev.*, **72**(1–2), 49–60.
- Geiss, J., et al. (1995b), The southern high-speed stream: Results from the SWICS instrument on ULYSSES, *Science*, **268**(5213), 1033–1036.
- Gloeckler, G., et al. (1998), Investigation of the composition of solar and interplanetary matter using solar wind and pickup measurements with SWICS and SWIM on the ACE spacecraft, *Space Sci. Rev.*, **86**(1–4), 492–539.
- Gosling, J. T., A. J. Hundhausen, and S. J. Bame (1976), Solar wind stream evolution at large heliocentric distances: Experimental demonstration and the test of a model, *J. Geophys. Res.*, **81**(13), 2111–2122.
- Gosling, J. T., D. N. Baker, S. J. Bame, W. C. Feldman, R. D. Zwickl, and E. J. Smith (1987), Bidirectional solar wind electron heat flux events, *J. Geophys. Res.*, **92**, 8519–8535.
- Gosling, J. T., J. Birn, and M. Hesse (1995), Three-dimensional magnetic reconnection and the magnetic topology of coronal mass ejection events, *Geophys. Res. Lett.*, **22**(8), 869–872.
- Gosling, J. T., R. M. Skoug, and W. C. Feldman (2001), Solar wind electron halo depletions at 90° pitch angle (2001), *Geophys. Res. Lett.*, **28**(22), 4155–4158.
- Gosling, J. T., R. M. Skoug, W. C. Feldman, and D. J. McComas (2002), Symmetric suprathermal electron depletions on closed field lines in the solar wind, *Geophys. Res. Lett.*, **29**(12), 1573, doi:10.1029/2001GL013949.
- Gosling, J. T., R. M. Skoug, D. J. McComas, and C. W. Smith (2005), Magnetic disconnection from the Sun: Observations of a reconnection exhaust in the solar wind at the heliospheric current sheet, *Geophys. Res. Lett.*, **32**, L05105, doi:10.1029/2005GL022406.
- Hirshberg, J., S. J. Bame, and E. E. Robbins (1972), Solar flares and solar wind helium enrichments: July 1965–July 1967, *Sol. Phys.*, **23**, 467–486.
- Howard, R. A., et al. (2008), Sun Earth Connection Coronal and Heliospheric Investigation (SECCHI), *Space Sci. Rev.*, **136**, 67–115.
- Kilpua, E. K. J., et al. (2009), Small solar wind transients and their connection to the large-scale coronal structure, *Sol. Phys.*, **256**(1–2), 327–344.
- Klein, L. W., and L. F. Burlaga (1982), Interplanetary magnetic clouds at 1 AU, *J. Geophys. Res.*, **87**, 613–624.
- Lepping, R. P., C. C. Wu, D. B. Berdichevsky, and T. Fergusen (2008), Estimates of magnetic cloud expansion at 1 AU, *Ann. Geophys.*, **26**, 1919–1933.
- Lockwood, M., R. Stamper, and M. N. Wild (1999), A doubling of the Sun's coronal magnetic field during the past 100 years, *Nature*, **399**(6735), 437–439.
- Luhmann, J. G., et al. (2008), STEREO IMPACT investigation goals, measurements, and data products overview, *Space Sci. Rev.*, **136**(1–4), 117–184.
- McComas, D. J., J. T. Gosling, J. L. Phillips, S. J. Bame, J. G. Luhmann, and E. J. Smith (1989), Electron heat flux dropouts in the solar wind: Evidence for interplanetary magnetic field reconnection?, *J. Geophys. Res.*, **94**, 6907–6916.
- McComas, D. J., S. J. Bame, P. Barker, W. C. Feldman, J. L. Phillips, P. Riley, and J. W. Griffiee (1998), Solar Wind Electron Proton Alpha Monitor (SWEPAM) for the Advanced Composition Explorer, *Space Sci. Rev.*, **86**(1/4), 563–612.
- Neugebauer, M., and R. Goldstein (1997), Particle and field signatures of coronal mass ejections in the solar wind, in *Coronal Mass Ejections*, *Geophys. Monogr. Ser.*, vol. 99, edited by N. Crooker, J. A. Joselyn, and J. Feynman, pp. 245–251, AGU, Washington, D. C.
- Opitz, A., et al. (2009), Temporal evolution of the solar wind bulk velocity at solar minimum by correlating the STEREO A and B PLASTIC measurements, *Sol. Phys.*, **256**, 365–377, doi:10.1007/s11207-008-9304-7.
- Owens, M. J. (2006), Magnetic cloud distortion resulting from propagation through a structured solar wind: Models and observations, *J. Geophys. Res.*, **111**, A12109, doi:10.1029/2006JA011903.
- Owens, M. J., N. A. Schwadron, N. U. Crooker, W. J. Hughes, and H. E. Spence (2007), Role of coronal mass ejections in the heliospheric Hale cycle, *Geophys. Res. Lett.*, **34**, L06104, doi:10.1029/2006GL028795.
- Owens, M. J., N. U. Crooker, and N. A. Schwadron (2008), Suprathermal electron evolution in a Parker spiral magnetic field, *J. Geophys. Res.*, **113**, A11104, doi:10.1029/2008JA013294.
- Pagel, C., N. U. Crooker, and D. E. Larson (2005), Assessing electron heat flux dropouts as signatures of magnetic field line disconnection from the Sun, *Geophys. Res. Lett.*, **32**, L14105, doi:10.1029/2005GL023043.
- Pilipp, W. G. H., M. D. Miggneried, D. Montgomery, K.-H. Muhlhauser, H. Rosenbauer, and R. Schwenn (1987a), Characteristics of electron velocity distribution functions in the solar wind derived from the helios plasma experiment, *J. Geophys. Res.*, **92**(A2), 1075–1092.
- Pilipp, W. G. H., M. D. Miggneried, D. Montgomery, K.-H. Muhlhauser, H. Rosenbauer, and R. Schwenn (1987b), Electron distribution functions in the solar wind derived from the Helios plasma experiment: Double strahl distributions and distributions with an extremely anisotropic core, *J. Geophys. Res.*, **92**(A2), 1093–1101.
- Rees, A., and R. J. Forsyth (2004), Two examples of magnetic clouds with double rotations observed by the Ulysses spacecraft, *Geophys. Res. Lett.*, **31**, L06804, doi:10.1029/2003GL018330.
- Rouillard, A. P., M. Lockwood, and I. Finch (2007), Centennial changes in the solar wind speed and in the open solar flux, *J. Geophys. Res.*, **112**, A05103, doi:10.1029/2006JA012130.
- Rouillard, A. P., et al. (2009a), A multispacecraft analysis of a small-scale transient entrained by solar wind streams, *Sol. Phys.*, **256**(1–2), 307–326.
- Rouillard, A. P., et al. (2009b), A solar storm observed from the Sun to Venus using the STEREO, Venus Express, and MESSENGER spacecraft, *J. Geophys. Res.*, **114**, A07106, doi:10.1029/2008JA014034.
- Sauvaud, J.-A., et al. (2008), The IMPACT Solar Wind Electron Analyzer (SWEA), *Space Sci. Rev.*, **136**(1–4), 227–239.
- Schwadron, N. A., L. A. Fisk, and T. H. Zurbuchen (1999), Elemental fractionation in the slow solar wind, *Astrophys. J.*, **521**(2), 859–867.
- Schwenn, R., and E. Marsch (1990), *Physics of the Inner Heliosphere*, *Phys. Chem. Space*, vol. 20, *Space and Solar Physics*, Springer-Verlag, Berlin.
- Sheeley, N. R., Jr., D. D.-H. Lee, K. P. Casto, Y.-M. Wang, and N. B. Rich (2009), The structure of streamer blobs, *Astrophys. J.*, **694**(2), 1471–1480.
- Smith, C. W., J. L'Heureux, N. F. Ness, M. H. Acua, L. F. Burlaga, and J. Scheifele (1998), The ACE Magnetic Fields Experiment, *Space Sci. Rev.*, **86**(1/4), 613–632.

- Snyder, C. W., M. Neugebauer, and U. R. Rao (1963), The solar wind velocity and its correlation with cosmic-ray variations and with solar and geomagnetic activity, *J. Geophys. Res.*, **68**, 6361–6370.
- van Aalst, M. K., P. C. Martens, and A. J. C. Belin (1999), Can streamer blobs prevent the buildup of the interplanetary magnetic field?, *Astrophys. J.*, **511**(2), L125–L128.
- Wang, Y.-M., and N. R. Sheeley Jr. (2003), On the topological evolution of the coronal magnetic field during the solar cycle, *Astrophys. J.*, **599**(2), 1404–1417.
- Wang, Y.-M., N. R. Sheeley Jr., J. H. Walters, G. E. Brueckner, R. A. Howard, D. J. Michels, P. L. Lamy, R. Schwenn, and G. M. Simnett (1998), Origin of streamer material in the outer corona, *Astrophys. J.*, **498**, L165–L168.
- Wang, Y.-M., N. R. Sheeley, D. G. Socker, R. A. Howard, and N. B. Rich (2000), The dynamical nature of coronal streamers, *J. Geophys. Res.*, **105** (A11), 25,133–25,142.
- Wang, Y.-M., Y. K. Ko, and R. Grappin (2009), Slow solar wind from open regions with strong low-coronal heating, *Astrophys. J.*, **691**, 760–769.
- Zurbuchen, T. H., S. Hefti, L. A. Fisk, G. Gloeckler, and R. von Steiger (1999), The transition between fast and slow solar wind from composition data, *Space Sci. Rev.*, **87**(1/2), 353–356.
- Zurbuchen, T. H., L. A. Fisk, G. Gloeckler, and R. von Steiger (2002), The solar wind composition throughout the solar cycle: A continuum of dynamic states, *Geophys. Res. Lett.*, **29**(9), 1352, doi:10.1029/2001GL013946.
- L. F. Burlaga, NASA Goddard Space Flight Center, Code 673, Greenbelt, MD 20771, USA.
- J. A. Davies, C. J. Davis, and R. A. Harrison, Space Science and Technology Department, Rutherford Appleton Laboratory, Fermi Ave., Chilton OX11 0QX, UK.
- R. J. Forsyth and N. P. Savani, Space and Atmospheric Physics Group, Blackett Laboratory, Imperial College London, London SW7 2BW, UK.
- A. B. Galvin and K. D. C. Simunac, Institute for the Study of Earth Oceans and Space, University of New Hampshire, Durham, NH 03824, USA.
- B. Lavraud, A. Opitz, and J.-A. Sauvaud, Universit de Toulouse, UPS, Centre d'Etude Spatiale des Rayonnements, Toulouse, France.
- M. Lockwood and A. P. Rouillard, Space Environment Physics Group, School of Physics and Astronomy, University of Southampton, Southampton SO17 1BJ, UK. (alexisrouillard@yahoo.co.uk)
- J. G. Luhmann, Space Science Laboratory, University of California, Berkeley, CA 94720, USA.